Advances in Water Resources 199 (2025) 104917

Contents lists available at ScienceDirect

Advances in Water Resources

journal homepage: www.elsevier.com/locate/advwatres

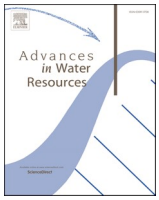

Two-dimensional capillarity-driven seepage from a lined buried ditch: The Kornev subsurface irrigation "Absorptional" method revisited

Anvar Kacimov [a,b,*], Yurii Obnosov [b,e], Tatyana Nikonenkova [c], Andrey Smagin [d,e]

[a] Department of Soils, Water and Agricultural Engineering, Sultan Qaboos University, Oman
[b] Institute of Mathematics and Mechanics, Kazan Federal University, Kazan, Russia
[c] Institute of Ecology and Geography, Kazan Federal University, Kazan, Russia
[d] Department of Soil Physics and Melioration, Faculty of Soil Sciences, Lomonosov Moscow State University, Moscow, 119991, Russia
[e] Institute of Forest Science, Russian Academy of Sciences, Uspenskoe, 143030, Russia

ARTICLE INFO

Keywords:
Capillary fringe
Tension-saturated seepage
Complex potential
Hodograph
Conformal mappings
HYDRUS2D modeling of buried ditches as subsurface irrigators
Constructozems

ABSTRACT

Kornev's (1935, see e.g. p.74, Fig. 34 - right panel) "open system" of capillarity-driven wetting of a fine-textured soil from a buried ditch filled by a coarse porous material is modeled analytically, using the methods of hodograph, and numerically, with the help of HYDRUS2D. Gravity, Darcian resistance of the soil at full saturation but negative pressure, and capillarity are three physical competing factors involved through the Vedernikov-Bouwer analytical model, which assumes 2-D, tension-saturated flow in a homogeneous soil sandwiched between the free surfaces (capillary fringe boundaries) and Kornev's impermeable liner of the ditch. Water seeps up from a line source, *viz*. a zero-pressure segment such that everywhere in the flow domain pressure remains negative. Lining minimizes deep percolation and facilitates upward and lateral spread of pore water by soil's capillarity. The free surfaces are streamlines, along which the pressure head is a negative constant (the air entrance pressure head, soil's property). For a small-depth ditch the hodograph domain is either a circular trigone, tetragon or sextagon, that determines three different flow topologies (with J.R.Philip's "dry shadow", "dry bulb" and no dry zone at all on the leeward side of the liner and "wet lobes" hanging on the edge of the liner). The flow domain makes a capillary "fountain". The complex potential domain is a half-strip such that the inversion method and conformal mappings are used. Transient, 2-D seepage in subsurface irrigation of a soil composite ("constructozem"), which consists of an ambient fine-textured soil and a buried Kornev's ditch (backfilled by a sand or peat), is numerically modeled by HYDRUS2D. Evapotranspiration is the fourth moisture-driving factor, which uplifts vadose zone moisture, combatting Pluto's gravity. The seepage flow rates, isobars, isohumes, isotachs, flow nets, vector-fields of Darcian velocity and other kinematic-dynamic seepage descriptors are found for various combinations of the physical properties of two contrasting porous materials and geometrical sizes (the width and depth of Kornev's ditch, depth of its burial, distance between neighbouring emitting ditches in a periodic irrigation system).

"The descent to Hades is the same from every place."

Anaxagoras

"A beautiful closed system,… its weakness totally shielded by its *strength*."

The Chronicles of Amber

1. Introduction

More than 30 % of the land of our planet with a population of 2 billion belongs to arid conditions with a high deficit of water resources, aggravated by global warming and increasing anthropogenic pressure (see e.g. Suleiman and Shahid, 2024, Zalibekov, 2011). Agricultural provision of food security, as well as the grandiose plans for the afforestation of the deserts, recently put forward by the leaders of the Gulf

Abbreviations: BVP, boundary value problem; CF, capillary fringe; FE, finite element; IBVP, initial boundary value problem; K-35, Kornev (1935), *Subsoil Irrigation (absorption irrigation method)*; Moscow, Selkhozgiz (in Russian); OS, open system; PK-62, *Theory of Ground-water Movement*; Princeton, *Princeton University Press*; Nauka, Moscow (in Russian); SI, subsurface irrigation; WUE, water use efficiency; WRC, water retention curve.

* Corresponding author at: Department of Soils, Water and Agricultural Engineering, Sultan Qaboos University Al-Khod 123, PO Box 34 Sultanate of Oman.
E-mail addresses: anvar@squ.edu.om (A. Kacimov), yobnosov@kpfu.ru (Y. Obnosov).

https://doi.org/10.1016/j.advwatres.2025.104917
Received 31 July 2024; Received in revised form 10 January 2025; Accepted 5 February 2025
Available online 11 February 2025

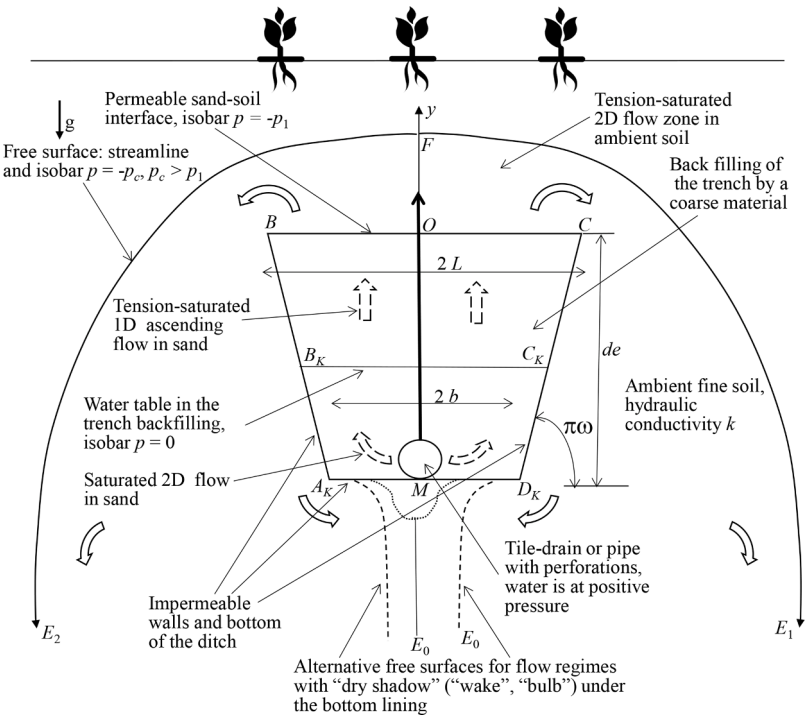

Fig. 1. Vertical cross-section of Kornev's SI, OS ditch acting as a "capillary fountain".

countries in connection with the green ESG agenda of the planet, require innovative technologies for irrigation and soil water conservation. Reduction of deep percolation and direction of pore water in the root zone upwards, towards transpiration, can be achieved by an intelligent soil design of so-called "constructozems" or layered-blocked soil composites, using the principle of controlled refraction of seepage flow paths at the boundaries between subzones with contrasting hydraulic properties, in particular, the phenomenon of the capillary barrier (Al-Maktoumi et al., 2014; Smagin, 2012). Constructozems based on peat, synthetic hydrogels and natural materials were successfully tested in UAE, Bahrain, Oman, Qatar, Uzbekistan and some other arid countries (Al-Maktoumi et al., 2014; Smagin and Sadovnikova, 2015; Smagin et al., 2022; Al-Mayahi et al., 2023; Deeb et al., 2024) and showed their efficiency and durability to extreme heats, mechanical impacts and biodegradation, with the 30–50 % increase in WUE, and reliable protection of root-inhabited topsoil from secondary salinization. Peat or hydrogel lenses imbedded into the "natural" urbisoils (subjacent to raingardens, swales, filter strips, mini-stands of wild plants on the banks of urban wadis winding through "concrete jungles" of the Gulf megalopolises) are now widely used even in Moscow and other Russian cities (see e.g. Smagin and Sadovnikova, 2015, Smagin et al., 2022), where, unlike the Gulf countries, the topology of the essentially non-1-D seepage through constructed porous media is determined by a season of snow melting in Springs, regular (rather than erratic) torrential rains and quite long droughts in Summers. The infiltrated pore water moves, along refracting streamline-pathlines-streaklines, through the natural, relatively fine-textured topsoil towards relatively coarse porous inclusions and then again refracting to deeper indigenous soil (Kacimov and Obnosov, 1995). Nowadays, the fine-textured lenses embedded in the soil profile at a given depth work as "invisible sponges" under green zones in some Russian urban and agricultural areas.

It is noteworthy that constructozems in modern urban and agricultural soil hydrology historically stem from kindred constructions practiced in subsurface irrigation (hereafter abbreviated as SI) used for cultivation of Soviet row crops. In the patent Kornev (1921) and seminal book Kornev (1935)[1] (abbreviated as K-35), two pioneering SI technologies were elaborated: a closed and open, which are operated under positive or negative pressure heads at the buried source of water supplied from an external tank. After Kornev, various SI techniques were used in arid-semiarid climates of the USSR (see e.g. Akhmedov et al., 2000, Astapov and Bobchenko, 1950, Barashkov, 1980, Bogushevsky, 1956, Bulakhtina et al., 2018, Glebov and Dementyev, 1966, Gostishev, 1980, Grigorov,1983, Kalashnikov et al., 2014, Kanardov, 1979, Karpii, 1980, Kichigin, 1958, Khamraev, 1974, 1980, Lunev and Khondroyanis, 1975, Mazepa, 1989, Nikiforov, 1936, Nikolaev, 1967, Readigger, 1965, Nasonov and Stanovov, 1978, Sheinkin, 1968, Ostapchik, 1961, Shumakov et al., 1985, Yakovlev and Razuvaev, 1982, Zakharov et al., 2021, Zavodnov and Morozov, 1962). A strategic aim was increasing the WUE (see e.g. Muromtsev, 1979).

Analytical models for 2-D Darcian seepage from SI sources were developed by Vedernikov (1939), Riesenkampf/Polubarinova-Kochina (1962, hereafter abbreviated as PK-62), Strack (1989), Philip (1989), among others. Kacimov and Obnosov (2017), Kacimov et al. (2018), Obnosov and Kacimov (2018) revisited and theorized seepage flows typical for Kornev's closed irrigation technology. In this paper, we study seepage in the Kornev open system (abbreviated as OS). K-35 explicated the agronomic and engineering details of his OS. In his publications, Kornev did not use mathematical models of pore water motion.[2]

OS in K-35 consists of a buried ditch filled with an imported coarse porous material (backfilling of the ditch). The ditch is surrounded by an ambient (indigenous) fine-textured soil. Fig. 1 shows a vertical cross-section of a trapezoidal ditch BA_kMD_kC (see also Figs. 26, 34, 37, 44,

[1] An electronic copy of the Kornev (1935) book is available as a Supplementary Electronic File.

[2] Relevant Richards', PK-62 and Vedernikov's boundary value problems (BVPs) to PDEs, which describe essentially 2-D Darcian unsaturated and saturated/tension-saturated flows in soils, were developed and tuned up after completion of Kornev's field projects, lab experiments and publication of his book.

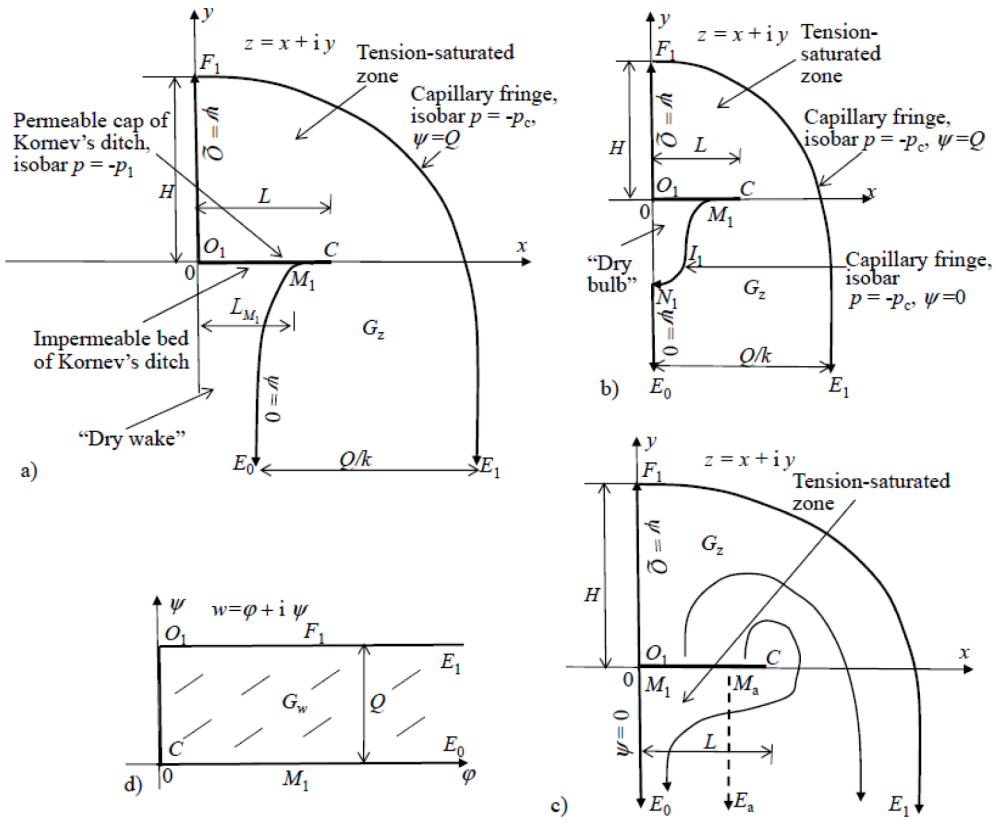

Fig. 2. Right halves of the vertical cross-section of physical domains G_z in case of mild capillarity (a), moderate capillarity (b) and critical capillarity (c). Complex potential domain G_w(d).

59, 61, 72, 76 in K-35).

The bottom (A_kMD_k) and side walls (BA_k and CD_k) of the ditch are impermeable (lined), the cap (BOC) of the backfilling is not lined, i.e. is a horizontal segment along which a good mechanical contact of the ditch filling with the soil is maintained. Water is supplied to the ditch through a perforated pipe placed on A_kMD_k. Depending on the variations of the pressure in the pipe, the water table (a horizontal segment B_kC_k in Fig. 1) inside the filling may vary but we assume it to be constant. Along B_kC_k the gage pressure head $p = 0$, in comport with the definition of the water table. Capillarity of the filling (although relatively small) drives water vertically up to another horizontal segment, along which $p = -p_{cf}$, where p_{cf} [cm] is a positive constant (the air-entrance pressure head of the filling). Obviously, the position of B_kC_k, controlled by the OS pipe operator should not be too small, because otherwise water will not be capillarity-hoisted to BOC, through which the ambient dry soil sucks water further up and laterally as is shown in Fig. 1a. On another hand, B_kC_k should not be too high because otherwise the pore water from the filling will extravasate from the confining trapezoidal liner in Fig. 1 and percolate down.

We recap: Capillarity of the filling in Fig. 1 drives water up to the horizontal segment BOC. From this line of a length $2L$ water is sucked by capillarity of the soil. The capillary rise inside the trapezium is almost vertical up, although near the emitting pipe in Fig. 1 seepage is 2D (Vedernikov, 1939, Project 3 in our Section 3). The capillary motion in the soil is everywhere essentially 2-D (see K-35 and Bobchenko, 1957).

Thus, using Strack's (1989) terminology, for the fine soil in Fig. 1 BOC is a horizontal line source of pore water driven up and laterally by soil's capillarity. The plant roots intercept this water from the wetted soil (and from the coarse ditch filling). Kornev's dream was to eliminate the gravity-driven (for Kornev gravity was Pluto's curse) descending seepage (deep percolation) beneath the ditch of his OS such that the irrigation water is used solely for transpiration (evaporation is minimized by a mulching or self-mulching, not shown in Fig. 1, viz. a layer of dry topsoil above the wetted zone in Fig. 1). Sadly, later experiments (see e.g. Bobchenko, 1957, 1959) showed that the pore water, which is not intercepted by the roots, still drains down, i.e. gets lost that is one the main drawbacks of any SI technology. Later analytical solutions (e.g. obtained by Philip, Childs, Raats, Warrick, Wooding, Youngs, and others) corroborated that the moisture uptake by plant roots, even facilitated by the capillary "dispersion" from a continuously emitting SI irrigation source, is an archenemy of the Newtonian gravity. Alas, evapotranspiration causes secondary salinization (not studied in K-35 and below). Various waterproof barriers to the downward seepage are now widely practiced in SI for all types of emitters (see e.g. El-Nesr, 2014, Goyal, 2014).

The purpose of this paper is to develop analytical and numerical solutions for flows from Kornev's OS lined ditch and to connect this SI with the theoretical legacy of Vedernikov (1939) and Riesenkampf (see PK-62), who worked with surface (e.g. furrow, border) irrigation projects. We answer the following questions:

- How much water is emitted from the line source BOC in Fig. 1?
- What is the size of the wetting zone?
- How significantly the impermeable (lined) part of the ditch contour reduces the downward gravitational "loss" of water to deep percolation as compared with the "upward drive" by capillarity?
- What is the impact of the contrast in hydraulic properties of the peat/sand filling of the ditch and ambient soil?
- Ontologically and theologically, is the hodograph method a right mathematical tool for confronting Pluto?

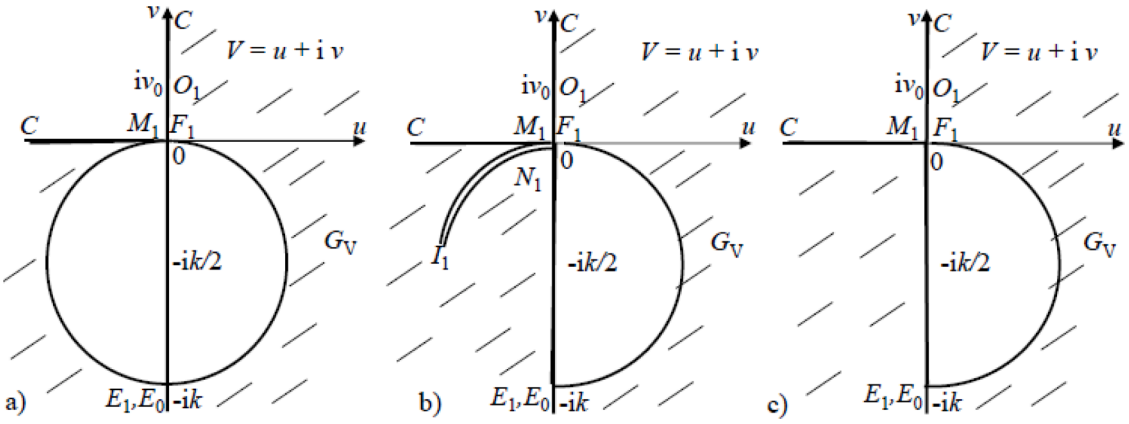

Fig. 3. Hodograph domains G_V (a-c) corresponding to G_z in Fig. 2a-c.

2. Analytical solution for capillary-tension flow from zero-depth[3] ditch

Due to symmetry, here and in Section 3 we consider the right half of flow from a ditch in Fig. 1. We also assume that the ditch is shallow, i.e. its depth $de = 0$ and therefore the water level there is negligible.

We introduce a complex coordinate $z = x + i\,y$ in the physical plane. Three regimes of seepage flows are shown in the vertical cross-sections, Fig. 2a-c. The flow domains are denoted G_z. In Fig. 2a-c, the ditch is modelled as a mathematical cut M_1CO_1. The top CO_1 of the cut is permeable and the bottom M_1C is impermeable that imitates Kornev's lining in Fig. 1. The "lined line emitter" in Fig. 2a-c is generalization of Zhukovsky's drain (see PK-62), which has both the top and bottom as equipotential/isobaric segments making a slot.

The total hydraulic head in steady-state seepage is defined as $h(x,y) = p(x,y) + y + p_1$. The specific discharge vector $\vec{V}(x,y)$ obeys Darcy's law $\vec{V}(x,y) = -k\nabla h$, where p is the pressure head and k is saturated hydraulic conductivity.

Three flow regimes are elaborated below. For all of them, a free boundary (the cap of the capillary fringe, abbreviated as CF) E_1F_1 (Fig. 2) is both a stream line and isobar $p = -p_c$, where p_c [cm] is a positive constant ($p_c > p_1$), tabulated in PK-62 and Vedernikov (1939) for typical ambient soils.

Everywhere inside G_z the pressure head is negative and bounded as $-p_c < p < -p_1$ but soil is under full saturation (k = const). We recall that Muromtsev (1991, p.137) distinguished three subdomains of the CF above a horizontal water table in various types of soils. Below we assume that our CF corresponds to Muromtsev's subdomain having 92–98 %% of saturation and "perfect hydraulic contact" (his parlance) within this subdomain.

In what follows, we assume (without any loss of generality) $p_1 = 0$. At infinity, $\vec{V}(x,-\infty) = v(x,-\infty) = -k$ that (in the vernacular of PK-62) corresponds to seepage without backwater (alternative regimes with backwater are discussed in Kacimov and Obnosov, 2023). Therefore, the free surfaces have vertical asymptotes. Consequently, at infinity the width of G_z is Q/k.

If soil's capillarity is mathematically zero ($p_c = 0$), then, obviously, water does not move up from O_1C in Fig. 2.

If capillarity is weak (small p_c), then the seepage topology is illustrated in Fig. 2a. The vertical streamline (separatrix in Fig. 1) OF_1 climbs up, attains its apex F_1 and, after that, makes a free surface FE_1. Evapotranspiration is ignored in all regimes in Fig. 2. Soil's thickness above OC_1 is large enough to disregard exfiltration of pore water on the surface that is sometimes visible by darkening of the soil above the SI buried lines. Another, "internal" free surface M_1E_0 clings to the liner and also descends to infinity. This curve is an interface between a tension-saturated flow zone and a "dry wake" (we use a modified J.R.Philip's terminology). Both FE_1 and M_1E_0 are concave up. The ordinate and abscissa of points M_1 and F_1, respectively, are not known.

If capillarity is stronger (large p_c), then the free surface under the liner becomes a finite-length curve $M_1I_1N_1$ shown in Fig. 2b. Point I_1 is an inflexion point. Points M_1 and N_1 are both stagnation points. A "dry bulb", sandwiched between M_1I_1 N_1 and the liner, is of a finite size.

At a certain critical value of p_c, the circular cut in Fig. 3b dwindles, the points M_1, I_1, and N_1 merge into one point M_1, i.e. the "dry bulb" under the liner (Fig. 2b) vanishes. The corresponding flow domain is shown in Fig. 2c.

We introduce a complex potential $w = \varphi + i\psi$, where $\varphi = -kh$ is the velocity potential and ψ is a stream function. Point O_1 is fiducial. Along O_1C in Fig. 2a-c, both p and h are constant and $\varphi = 0$ there. The flow rate Q (per unit length perpendicular to the z-plane) in G_z is to be found ($\psi = 0$ along CM_1E_0 and $\psi = Q$ along $O_1F_1E_1$). Therefore, the complex potential domain, G_w, is the same half-strip (Fig. 2d) for all three flow regimes in Fig. 2a-c.

A "dry shadow" beneath point M in Fig. 1 is shown by dotted and dashed curves. We note that in large canals (designed for conveying surface water rather than for irrigation of adjacent soil, see e.g. Kacimov, 1992, Subramanya et al., 1973, Swamee and Chahar, 2015) seepage with a "dry shadow" beneath a bottom lining is considered as a loss. In such channels, lining of the bottom, banks or the whole wetted perimeter (and even the free board part of the slopes) is an expensive means for reducing this loss. Intricate "dry shadows", "wet lobes and kippahs/כיפה" on the stoss-, lee –sides of subsurface stones, tunnels, subterranean holes, silos of ICBMs, etc. emerge due to transformation of trivial 1-D unsaturated or tension-saturated descending seepage to a whimsical 2-D one, in terms of both the Vedernikov-Bouwer and quasilinear analytical models (see e.g. Kacimov, 2000, 2007, Kacimov and Nikolaev, 1992, Kacimov et al., 2019, 2022, Philip et al., 1989, Samal and Mishra, 2022).

Kornev's OS, as a SI technology, is subtle: a part (BOC in Fig. 1) of the wetted perimeter of the buried ditch must be open for seepage and moisture supply to plants' roots. These roots may grow under A_kMD_k in Fig. 1 and eliminate the deep percolation by interception of all water seeped from the SI emitter. That would be an ideal scenario from the view point of WUE.

We introduce a complex specific discharge $V = u + iv$, where $u(x,y)$ and $v(x,y)$ are its horizontal and vertical components. The hodograph domains, G_V, corresponding to seepage regimes in Fig. 2a-c, are shown in Fig. 3a-c. In Fig. 3a, G_V is a circular trigon, viz. a complex plane from which two areas are excluded: the upper left quadrant and the interior of a circle of a radius k and centered at the point $V = -i\,k/2$. These areas are

[3] All Wolfram's *Mathematica* programs are open sources and are available upon request.

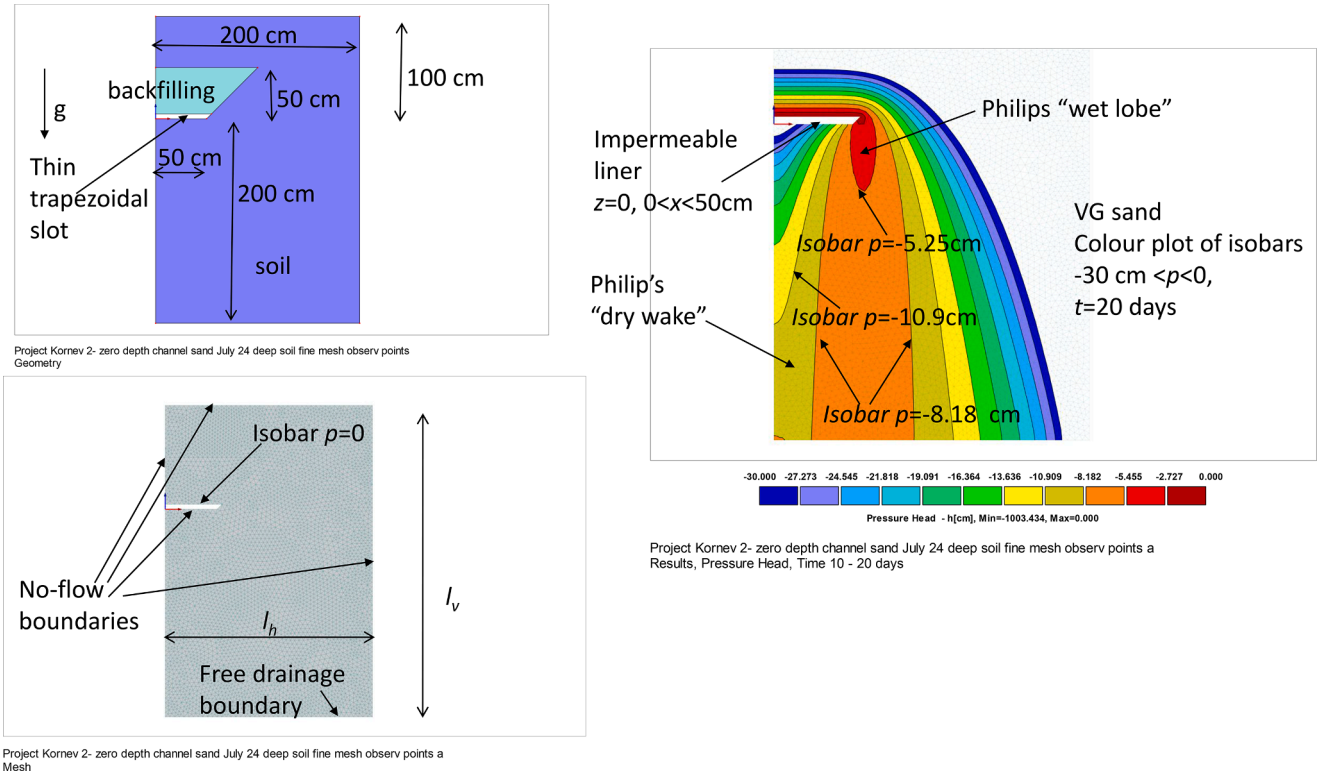

Fig. 4. HYDRUS flow domain (left upper panel) with a shallow trapezoidal slot with a lined bed, boundary conditions and FE mesh (left lower panel), isobars in VG sand for a quasi-steady seepage (right panel).

not shaded in Fig. 3a. In Fig. 3b, G_V is a circular sextagon, viz. a complex plane from which two areas are excluded: the upper left quadrant and the interior of a half-circle. This G_V has a circular cut $M_1I_1N_1$ (a circular arc of a radius k and centered at the point $V = -i\,k/2$). In Fig. 3c, G_V is a degenerate case of one in Fig. 3b, in which the circular cut has vanished. If one uses the Riemann sphere, then the "infinities" in G_z are imaged by a single point but in Fig. 2 we distinguish the ends of the vertical asymptotes. Also in G_V domains (Fig. 3), the stagnation points F_1, M_1 and N_1 (collapsing to the same point on the corresponding Riemann sphere) are distinguished by placing them on opposite sides of the corresponding cuts (notice, for example, an infinitesimally small "gap" between F_1 and M_1 in G_V). We use a common convention in the theory of holomorphic functions: a walk around a domain in a complex plain is positive if the domain remains on the right.

It is noteworthy that due to the presence of a horizontal streamline segment M_1C_1 the image of G_z in the plane of the Zhukovsky function (used in Kacimov, 2004, 2006) becomes neither a polygon nor a circular polygon.

In the Appendix we use methods of the theory of holomorphic functions (Henrici, 1993) and solve the flow problem for the special (critical) case in Fig. 2c- 3c and for the case with a "dry shadow" behind the liner, which corresponds to Fig. 2a-3a.

3. HYDRUS2D[4] simulations

In this Section, numerical (FE method) modeling, viz. solution of the Richards-Richardson (abbreviated as RR) PDE with the help of HYDRUS package (see e.g. Radcliffe and Šimůnek, 2018 for more details) is exemplified. Unlike Section 2, where seepage was steady state and the Vedernikov-Bouwer model reduced the RR PDE to the Laplace PDE, for which BVPs are solved by various methods of the theory of holomorphic functions (PK-62, Strack,1989), below we deal with transient seepage (time, t, is an independent physical variable). HYDRUS solves 2D initial boundary value problems (IBVP), for which no analytical solutions are available.

Project 1. We start with an IBVP for SI OS, which geometrically and in the asymptotic limit $t \to \infty$ is close to one in Section 2, regime in Fig. 2a. Fig. 4 illustrates the right half of a HYDRUS flow domain, which is a rectangle having a horizontal and vertical sizes $l_h = 200$ cm and $l_v = 300$ cm, respectfully. Therefore, physically the distance between the axes of Kornev's ditches (periodic-systematic SI of row crops, like maize in K-35) is 400 cm. A trapezoidal backfilled Kornev's ditch has the bed width of 50 cm, the depth of 50 cm and 1:1 slope (the bank slope angle in Fig. 1, $\omega = 1/4$). The origin of HYDRUS Cartesian coordinates (xOz in this Section) is at the midpoint of the trapezium bed such that the soil surface is at the horizon $z = 100$ cm and the free drainage horizon is at $z = -200$ cm.

To approximate the analytical solution in Section 2, we made a bed cut in Fig. 4. Specifically, in the HYDRUS geometry we made a cut as a thin "white" trapezium of a height of 4.75 cm. The top of this trapezium is at the boundary condition $p = 0$, the bottom (a segment of a width of 50 cm) and tiny slope are HYDRUS no-flow boundaries. Physically, such conditions mean that the water level of 4.75 cm is maintained in the ditch by continuously injecting water into it from an external tank, as K-35 did in his OS irrigated crop fields. Other boundary conditions are indicated in Fig. 4, in particular, the segment $Z = 100$ cm is a no flow boundary, i.e. we ignore evaporation from the soil surface.

In Project 1, we assume that the ambient soil and backfilling are made of the same Van Genuchten (VG) sand (see the HYDRUS soil catalogue, i.e. the VG capillarity parameters are $\alpha = 0.1451$/cm and $n = 2.68$). The finite element size is 4.5 cm such that the mesh discretization parameters are: 4627 nodes, 9008 2D and 280 1D elements.

The initial ($t = 0$) condition in the whole flow domain is $p = -50$ cm that corresponds to an almost irreducible volumetric moisture content θ_r

[4] All HYDRUS2D projects are open sources and are available upon request.

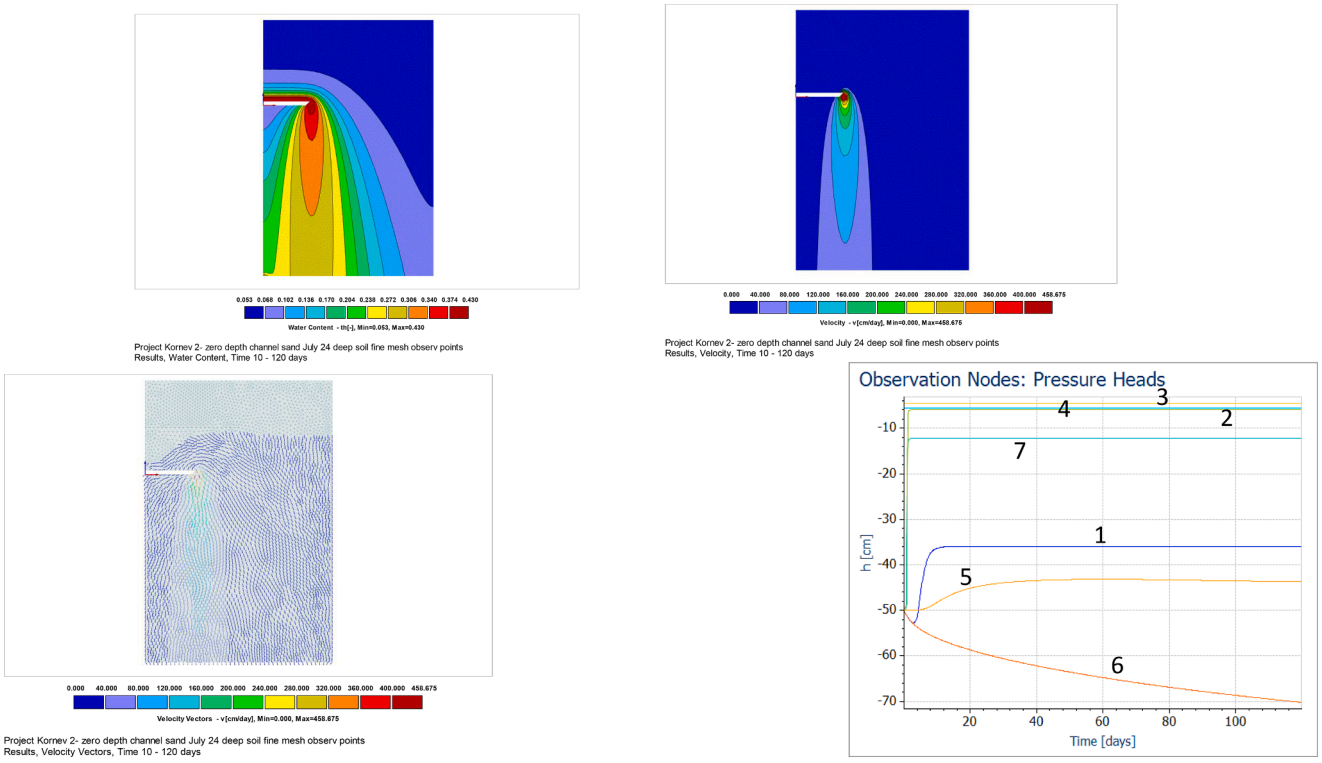

Fig. 5. Volumetric moisture content (upper left panel), isotachs (upper right panel), vector field of Darcian velocity (lower left panel) and pressure head variation with time at seven observational points for thin trapezoidal slot having impermeable bed and $p = 0$ roof.

$= 0.045$ of the VG sand. At $t = 0$ the top of the trapezoidal thin slot is subject to the boundary condition $p = 0$ and moisture starts moving from this slot to the sand. The total simulation time is 120 days, although Q (the upward inlet flow rate from a line source which gets almost equal to the downward rate through the outlet of the free drainage boundary) attains its steady state at about $t = 20$ days.

The right panel in Fig. 4 demonstrates the palette of isobars, plotted in the range -30 cm $< p < 0$. The isobar $p = -8.18$ cm has two branches. The right one corresponds to the analytical curve F_1E_1 in Fig. 2a. The left branch of this HYDRUS isobar corresponds to the analytical curve M_1E_0 in Section 2. The analytical and numerical curves are close to each other.

Of course, if we dilate the HYDRUS flow domain, for example, by moving the free drainage (outlet) boundary $Z = -200$ cm in Fig. 4 to a sufficiently deep level, then the isobar $p = -8.18$ cm will be a one-branch oval-shaped curve similar to the isobar $p = -5.25$ cm in Fig. 4. In this sense, the analytical and numerical solutions do not match because the free boundaries $p = -p_c$ in Section 2 have vertical asymptotes at Pluto's infinity (clearly, as any other numerical package, HYDRUS operates with finite size domains only). The HYDRUS steady-state flow rate $Q_H = 5284$ cm^2/day that in dimensionless quantities of Section 2 is about 0.15, which is reasonably close to $Q = 0.21$ in the analytical solution. The discrepancy can be caused by the difference in the two

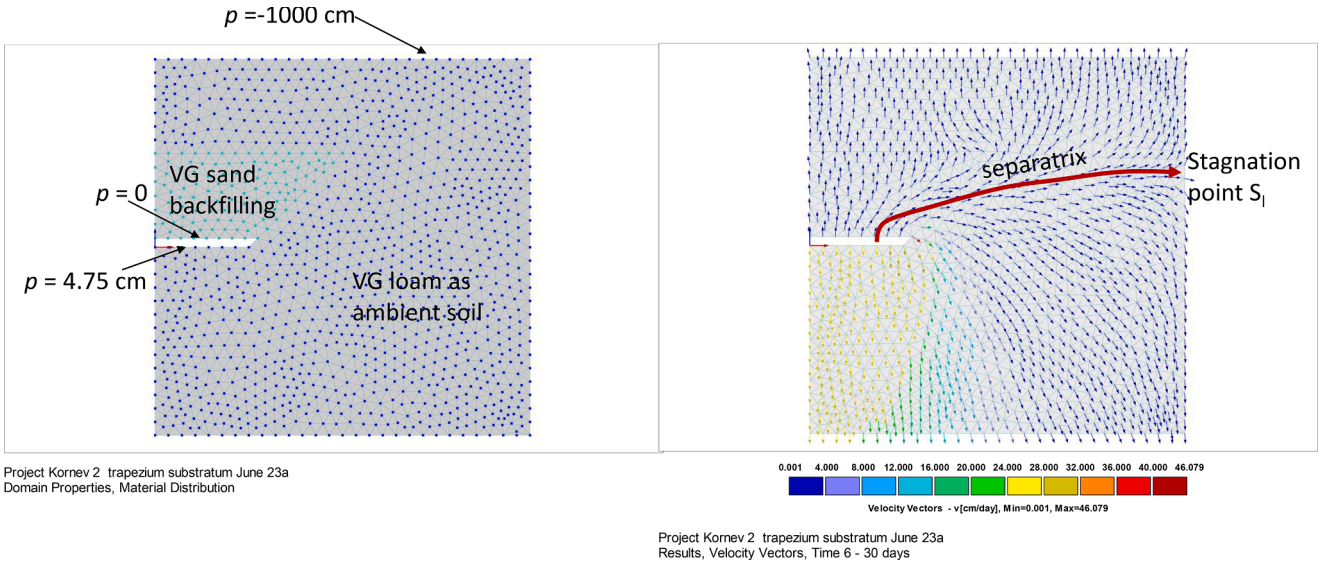

Fig. 6. FE triangulation and nodes for a sand-loam composite, unlined bed of Kornev's ditch and 4.75 cm water level at the ditch bed; vector-field of Darcian velocity with a part of exfiltrated water hoisted to a dry soil surface, a separatrix and additional stagnation point S_r.

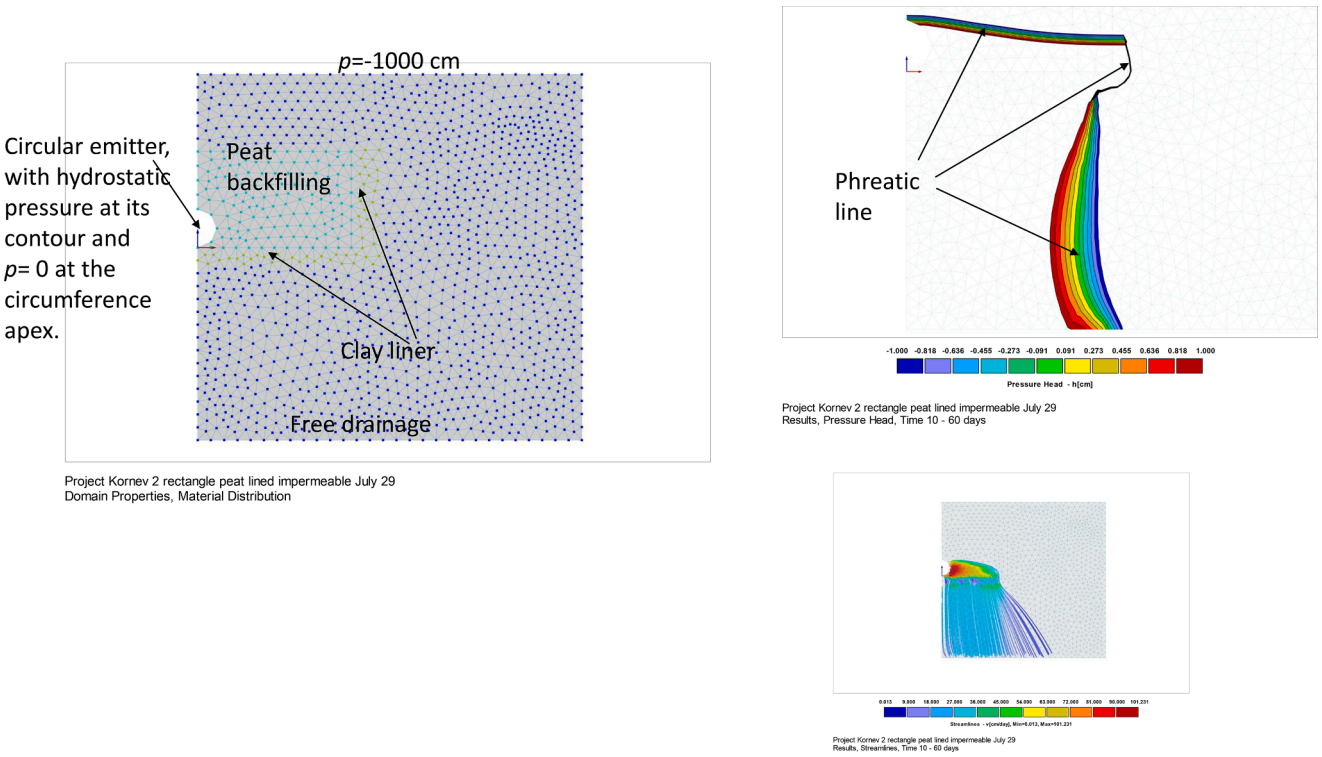

Fig. 7. Triangulated HYDRUS flow domain with K-35 perforated pipe emitting water into a peat-filled rectangular ditch with VG's clay as a bed and side liner (left panel); phreatic lines (right upper panel); streamlines (right lower panel).

permeability models: maximum (a saturated hydraulic conductivity of VG's saturated $k = 712.8$ cm/day in the whole tension-saturated flow domain of Section 2 and VG's relative permeability decreasing with the degree of saturation in the RR PDE).

In Fig. 5 we present the $t = 120$ days snapshots: the $\theta(x,z)$ colour map (upper left panel), isotachs (upper right panel), and the vector field of Darcian velocity (lower left panel). Obviously, at the right tip of the "white slot" the velocity magnitude attains very high values (infinite in the analytical solution). J.R.Philip would be glad to see the "wet lobes" in Figs. 4 and 5, which "hang" on the tip of the liner.

We also placed seven HYDRUS observational points 1–7 having the coordinates: (0,0), (0,−100 cm), (0,−200 cm), (0,10 cm), (0.50 cm), (0,100 cm), (100 cm, 0), correspondingly. The correspondingly numbered curves, pressure head variations $p(t)$, are shown in Fig. 5, right bottom panel. We notice that at the uppermost points 5 and 6, p has not reached a steady state limit (no horizontal asymptotes of $p(t)$ in Fig. 5) in 120 days.

For the sake of brevity, we skip over the sensitivity analysis, in which we truncated-expanded the flow domain (Fig. 4) from the right (the size of an elementary cell in the K-35 periodic SI) and from the bottom, changed the initial conditions for p, varied the triad of the VG constants (α, n, k) (see e.g. Al-Mayahi et al., 2023 for the protocols of such analysis).

Project 2. Now we consider seepage from a trapezoidal ditch backfilled with the VG sand (Fig. 6). We recall that the HYDRUS catalogue reports (α, n, k) = (0.036 1/cm, 1.56, 25 cm/day) for this porous medium. The VG loam is an ambient soil, i.e. we model a porous composite made of two soils contacting each other through the contour of a thin trapezium in Fig. 6. The bottom of the ditch is now not lined and the pressure head boundary conditions along the thin trapezoidal slot in Fig. 6 indicate a hydrostatic pressure and total heads along the three boundaries of this cut. The initial condition now is the default HYDRUS one, i.e. $p = -100$ cm. Also, the topsoil boundary condition is $p = -1000$ cm, i.e. a pretty high dryness is imposed (we recall that J.R.Philip considered the regime of absolute dryness of the topsoil as "the worse" in the sense of secondary salinization in SI). The mesh is coarser than in Project 1 and the flow domain is "shorter", viz. $l_v = l_h$ 300 cm (this reduces the time of HYDRUS computations). A snapshot of the vector field of the Darcian velocity at $t = 30$ days (an almost steady-state seepage) is shown in Fig. 6 (right panel). As compared with a simple "flow tube" (one inlet and one outlet) in Project 1, Fig. 6 demonstrates a more complex topology: a separatrix (only schematically sketched) is a watershed boundary between what seeps from the thin slot of positive pressure to the atmosphere and what descends to deep percolation. A stagnation point S_r at the right boundary of the flow domain has an ordinate $y = 36$ cm. The total free drainage (deep percolation) flow rate $Q_H = 2.05\times10^3$ cm^2/day. In Fig. 6, the highest magnitudes of velocity are close to a "triple point", the vertex of the thin trapezium, at which "free water" in the ditch is in contact with both porous media (sand and loam). Kacimov and Obnosov (2012) showed that at these "singular" points seepage erosion may cause major damage to the interior of hydraulic structures, where zones of contrasting hydraulic conductivity and porosity are in contact.

Project 3. In this HYDRUS project, we considered a rectangular ditch, the half of which (Fig. 7, left panel) is 40 cm wide and 25 cm tall. Backfilling is peat. Hydraulic properties of peats are reported elsewhere, e.g. by Boelter and Verry (1977), Efimov (1983), and Päivänen (1973). In our HYDRUS computations, we assume that the pentad of VG parameters for peat is: $k_{peat} = 480$ cm/day, $\alpha = 0.0381$/day, $n = 1.216$, $\theta_s = 0.916$, $\theta_r = 0.02$. These parameters are taken from Smagin et al. (2023) for the backfilling of the lenses in HYDRUS-1D designed experimental constructozems for blue spruce seedlings (*Picea pungens* Engelm) in the Serebryanoborsky forestry of the Russian Academy of Sciences, Moscow.

The corresponding WRCs were obtained by the centrifugation method in a modification (Smagin et al., 2023), taking into account the effect of gravity at low centrifuge rotation speeds. A circular emitter in

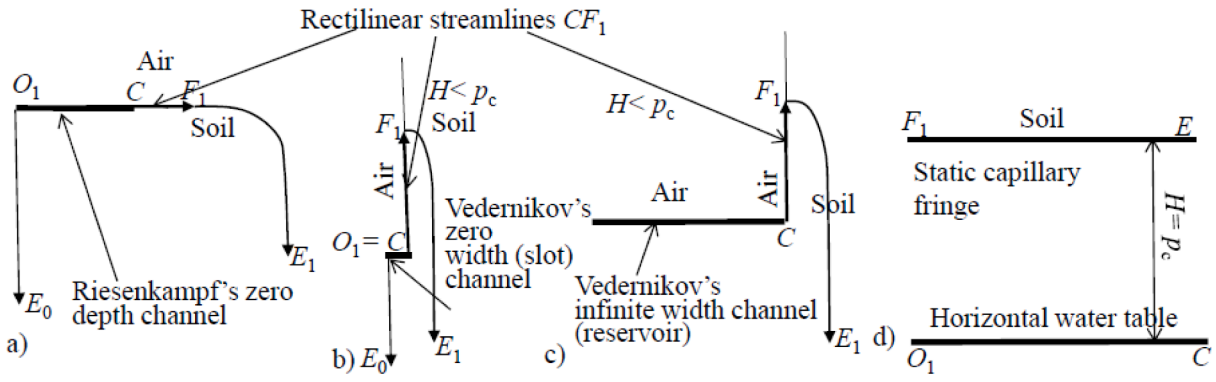

Fig. 8. . Schematic seepage topology from non-lined zero-depth surface water bodies (a-c) and horizontal water table with a horizontal capillary fring (d) in soils obeying the Veernikov-Bouwer CF model: a) Riesenkmapf's finite-width channel, b) Vedernikov's vertical slot, c) Vedernikov's reservoir.

Fig. 7 models Kornev's pipe A_kMD_k (see Fig. 1, Section 1) of a radius of 5 cm, which is placed at the bottom of the backfilling. The ambient soil is the VG loam. The bed of the ditch is lined -again imitating K-35 design - by the VG clay (in HYDRUS, the pentad of clay's hydraulic parameters is $k_{clay} = 0.1$ cm/day, $\alpha = 0.008$/day, $n = 1.09$, $\theta_s = 0.38$, $\theta_r = 0.068$). The liner thickness is about 4 cm. Therefore, in this Project we model a three-component porous composite.

The initial conditions are the default HYDRUS ones. The boundary condition along the emitter contour is hydrostatic pressure with $p = 0$ at the apex of the semi-cricle in Fig. 7, left panel. Other boundary conditions are the same as in Project 2.

In Fig. 7 (upper right panel), we plotted (at t = 60 days, almost steady-state seepage) the isobars in a narrow range -1 cm $< p <$ 1cm. These isobars sandwich the phreatic line. Owing to seepage, the upper part of this line in the peat is a sigmoidal curve. It is depressed from the axis of symmetry towards the side of the peat-filled rectangle. A phreatic line under the ditch liner separates a positive pressure zone on the left from a negative pressure zone on the right. Thus, the phreatic line in Fig. 7 is not only "inverted" but also intricate and serpentine.

The streamlines are also plotted in Fig. 7 (lower right panel). The total flow rate through the free drainage outlet is: $Q_H = 1.233\times10^3$ cm^2/day.

4. Concluding remarks and perspectives

The analytical solution in Section 2 is a new analytic element (Strack, 1989), a kind of "inversion" of Riesenkampf's one for seepage from a zero-depth channel with capillarity, depicted in Fig. 8a (see PK-62, pp.162–166, for the details of Riesenkampf's work).

Indeed, in Riesenkampf's case water seeps vertically down from a zero-pressure isobar of a finite length L, laterally to the right and eventually again down, i.e. the internal streamline shown in Fig. 8a is sigmoidal. Riesenkampf's horizontal streamline segment, which separates the tension-saturated soil and air, connects a horizontal equipotential line with a free surface, along which $p = -p_c$. In our case in Fig. 2, water particles emitted from a zero-pressure isobar move first vertically up, then laterally rightward and eventually gravity drives them vertically down. Moreover, a horizontal barrier O_1 M_1 in Fig. 2 forces the pore water under this lining (i.e. at negative y values) to move leftward. Consequently, the hodograph domains in Fig. 3 are more complex than the Riesenkampf one. Fig. 8b illustrates the limit $L = 0$, which represents the case of Vedernikov's slot-emitter, in which the water level is small. Water seeps horizontally through the permeable vertical bank of the slot and turns down 90°, when moving to infinity. All streamlines are concave up (no inflexion points). Flow in Fig. 8b is also a limit of Vedernikov's (1936, 1940) seepage from a trapezoidal canal. Fig. 8c depicts the limit $L = \infty$. Here water particles close to the vertical bank seep vertically down from a shallow reservoir, then up, rightwards (driven by capillarity) and eventually vertically down. Fig. 8d represents the degenerate case of a horizontal water table and a horizontal cap of the CF. Obviously, water is static in such system (provided, of course, no evaporation from the soil surface).

HYDRUS2D pore water modeling is versatile in the sense of the geometry of SI, initial, boundary conditions and heterogeneity of the soil, backfilling and liner of Kornev's OS. Numerical results for solving the RR PDE match the analytical ones for steady-state limits.

CRediT authorship contribution statement

Anvar Kacimov: Writing – review & editing, Writing – original draft, Visualization, Validation, Software, Resources, Project administration, Methodology, Investigation, Funding acquisition, Formal analysis, Conceptualization. **Yurii Obnosov:** Writing – review & editing, Visualization, Validation, Investigation, Formal analysis. **Tatyana Nikonenkova:** Investigation. **Andrey Smagin:** Writing – review & editing, Validation, Resources, Project administration, Investigation, Funding acquisition, Conceptualization.

Declaration of competing interest

The authors declare that they have no known competing financial interests or personal relationships that could have appeared to influence the work reported in this paper.

Acknowledgements

This work was funded by SQU, grants IG/AGR/SWAE/22/02, IG/VC/WRC/21/01, DR/RG/17 and by Russian Scientific Foundation, interdisciplinary project no 23-64-10002. Helpful comments by two anonymous referees are appreciated.

Supplementary materials

Supplementary material associated with this article can be found, in the online version, at doi:10.1016/j.advwatres.2025.104917.

Appendix. Details of analytical solution

Critical seepage topology

The boundary-value problem (BVP) for a holomorphic function $w(z)$ is:

$$\begin{aligned}&\psi = Q \text{ along } O_1F_1,\\ &\psi = Q, \quad \varphi/k + y = p_c \text{ along } F_1E_1,\\ &\psi = 0 \text{ along } M_1C\ (y=0) \text{ and } E_1M_1\ (x=0),\\ &\varphi = 0 \text{ along } CO_1\ (y=0).\end{aligned} \tag{A1}$$

In (A1) a linear combination of real or imaginary parts of two complex functions, z and w, is given along the domain boundaries (including the free one). The function $V(z)$ is anti-holomorphic and hence we introduce a holomorphic function $\omega = u - iv = dw/dz$. G_ω is the domain symmetric with G_V about the real axis (Fig. A1a). We use the method of inversion (see e.g. PK-62, Samal and Mishra, 2017, 2022), which works for circular polygons whose boundaries (circular arcs and straight lines) intersect at one point (the origin of coordinates in Fig. A1a for our case), i.e. we inverse G_ω with respect to the point F_1 (M_1). We get a regular tetragon G_{ω_1} (Fig. A1b) in the plane $\omega_1 = 1/\omega$.

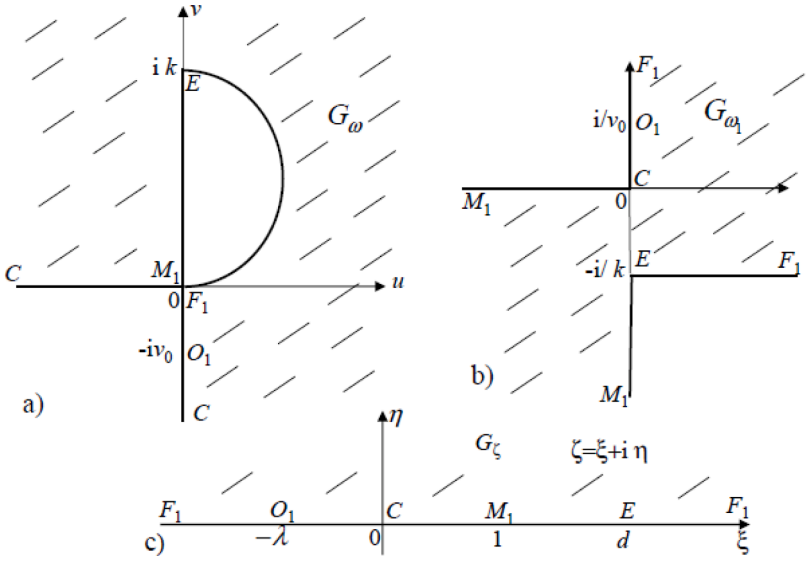

Fig. A1. Domain G_ω, a mirror image of G_V with respect to the Ou axis (a), inverted hodograph G_{ω_1} (b), auxiliary reference plain (c).

We map conformally G_{ω_1} onto an upper half-plane G_ς (Fig. A1c) of a reference plane $\zeta = \xi + i\eta$ by the Schwartz-Christoffel formula:

$$\omega_1(\varsigma) = -\frac{1}{c}\int_0^\varsigma \frac{\sqrt{t(d-t)}}{(1-t)^{3/2}}dt = -\frac{I(\varsigma)}{c}. \tag{A2}$$

where the real constants of the mapping, *viz.* the coefficient $c > 0$ and accessory parameter $d > 1$, are found below.

Integrating by parts in Eq. (A2), we get

$$I(\varsigma) = 2\sqrt{\frac{\varsigma(d-\varsigma)}{1-\varsigma}} + \int_0^\varsigma \frac{\sqrt{t}dt}{\sqrt{(d-t)(1-t)}} - \int_0^\varsigma \frac{\sqrt{d-t}dt}{\sqrt{t(1-t)}}. \tag{A3}$$

The branches of all radicals (multivalued functions) in Eq. (A3) are fixed in the upper half of the ς-plane by the condition of theirs positiveness at the interval $\xi \in (0,1)$.

We introduce dimensionless quantities: (z^*, w^*, V^*, Q^*, H^*, p_c^*,c^*)= (z/L, $w/(k\,L)$, V/k, $Q/(k\,L)$, H/L, p_c/L, c/k) and – for the sake of brevity - drop the superscript "*".

The condition $\omega_1(d) = -i$ (see Fig. A1b) gives two relations:

$$\mathrm{Re}\omega_1(d) = 0, \qquad \mathrm{Im}\omega_1(d) = -1. \tag{A4}$$

It is noteworthy that the condition at infinity (point E on the Riemann sphere) and the asymptotic behavior in the physical plane of Fig. 2 is $v = -k$ that is an analogue of "free drainage" in HYDRUS. PK-62 elaborates that in the analytical model for flow domains unbounded from below the only alternative of such condition at point E is $v = 0$.

Clearly, both integrals in Eq. (A3) are real for $0 < \varsigma < 1$ and purely imaginary at the interval $(1,d)$. Correspondingly, the first condition in (A4) is a nonlinear equation for determination of d:

$$\int_0^1 \frac{\sqrt{t}\mathrm{d}t}{\sqrt{(d-t)(1-t)}} - \int_0^1 \frac{\sqrt{d-t}\mathrm{d}t}{\sqrt{t(1-t)}} = 0. \tag{A5}$$

Eq. (A5), upon integration, may be written as

$$2\sqrt{d}(\mathrm{K}(1/d) - 2\mathrm{E}(1/d)) = 0,$$

where E and K stand for the complete elliptic integrals of the first and second kind, respectively (Abramovitz and Stegun, 1970).

From the second relation (A4) and Eqs. (A2), (A3) we find that

$$c = c(d) = \int_1^d \frac{(2t-d)\mathrm{d}t}{\sqrt{t(t-1)(d-t)}},$$

or, using the substitution $(t-1)/t = (1-1/d)\tau$, we get upon integration

$$c(d) = 2\sqrt{d}(2\mathrm{E}(1-1/d) - \mathrm{K}(1-1/d)). \tag{A6}$$

We used Wolfram (1991) *Mathematica* routines **FindRoot, NIntergate, EllipticK, EllipticE** for calculation of d and c from Eqs. (A5) and (A6). Computations yield:

$$d \approx 1.2105, \qquad c \approx 2.9784. \tag{A7}$$

Eventually, the mapping function is

$$\omega(\varsigma) = -c\left(2\sqrt{\frac{\varsigma(d-\varsigma)}{1-\varsigma}} + \int_0^{\varsigma} \frac{2t-d}{\sqrt{t(1-t)(d-t)}}\mathrm{d}t\right)^{-1}, \tag{A8}$$

where c and d are specified in Eq. (A7).

We now map G_w and G_ζ onto each other, again by the Schwartz-Christoffel formula:

$$\varsigma(w) = \lambda d\frac{\cosh\frac{\pi w}{Q} - 1}{\lambda\cosh\frac{\pi w}{Q} + 2d + \lambda}, \qquad w(\varsigma) = \frac{Q}{\pi}\operatorname{arcosh}\frac{(2d+\lambda)\varsigma + \lambda d}{\lambda(d-\varsigma)}. \tag{A9}$$

We differentiate $w(z)$ in Eq. (A9) and obtain

$$w'(\varsigma) = \frac{Q}{\pi}\frac{\sqrt{d(d+\lambda)}}{(d-\varsigma)\sqrt{\varsigma(\varsigma+\lambda)}}. \tag{A10}$$

We use Eqs. (A2), (A3) and (A10) to integrate

$$z(\zeta) = \int_0^{\zeta} \frac{\mathrm{d}z}{\mathrm{d}w}\frac{\mathrm{d}w}{\mathrm{d}\tau}\mathrm{d}\tau + 1 = \frac{Q\sqrt{d(d+\lambda)}}{\pi}\int_0^{\zeta} \frac{\omega_1(\tau)\mathrm{d}\tau}{(d-\tau)\sqrt{\tau(\tau+\lambda)}} + 1, \tag{A11}$$

where we took into account the condition $z(0) = 1$ (see Fig. 2c). Obviously, $z(-\lambda) = z(1) = 0$ and from Eq. (A11) follows:

$$\int_{-\lambda}^{0} \frac{\mathrm{d}w}{\mathrm{d}\zeta}\omega_1(\zeta)\mathrm{d}\zeta = 1, \int_0^1 \frac{\mathrm{d}w}{\mathrm{d}\zeta}\omega_1(\zeta)\mathrm{d}\zeta = -1. \tag{A12}$$

We note that both Eqs. (A12) are essential because they determine the flow regime shown in Fig. 2c. Indeed, the hodograph domain in Fig. 3c describes seepage with a vertical streamline along a ray M_aE_a (a dashed arrowed ray in Fig. 2c), i.e. the flow domain alternative to Kornev's one in Fig. 2c. Mathematically, a vertical ray M_aE_a is possible but physically (sedimentologically or geomorphologically) such a "vertical wall" is highly unlikely to exist in the subsurface.

First, from Eqs. (A12) we eliminate Q and get the following equation for determination of the accessory parameter λ:

$$\int_{-\lambda}^{1} \frac{\omega_1(\tau)\mathrm{d}\tau}{(d-\tau)\sqrt{\tau(\tau+\lambda)}} = 0. \tag{A13}$$

The solution of Eq. (A13) with the help of the **FindRoot** routine results in $\lambda = 14.315$. Next, we find Q using any one of two Eqs. (A12) where the parameters λ, c, and d are already found:

$$Q = \frac{\pi}{\sqrt{d(d+\lambda)}}\Big/\int_{-\lambda}^{0} \frac{\omega_1(\tau)\mathrm{d}\tau}{(d-\tau)\sqrt{\tau(\varsigma+\tau)}} = \frac{-\pi}{\sqrt{d(d+\lambda)}}\Big/\int_0^1 \frac{\omega_1(\tau)\mathrm{d}\tau}{(d-\tau)\sqrt{\tau(\varsigma+\tau)}}. \tag{A14}$$

Eq. (A14) yields $Q \approx 2.365$. From Eq. (A11), we have

$$H = \mathrm{Im}z(-\infty) = \frac{Q\sqrt{d(d+\lambda)}}{\pi}\int_{-\lambda}^{-\infty}\frac{\mathrm{Im}\omega_1(\zeta)\mathrm{d}\zeta}{(d-\varsigma)\sqrt{\varsigma(\varsigma+\lambda)}} = 1.3679. \tag{A15}$$

The improper integral in Eq. (A15) has the behavior $\omega_1(\varsigma) = \mathrm{O}\left(\sqrt{\varsigma}\right)$ in the vicinity of infinity.

Point F_1 is on the free surface and, therefore, we get from Eq. (A9):

$$H = p_c - \frac{Q}{\pi}\mathrm{Re}\left(\mathrm{arccosh}\frac{2d+\lambda}{-\lambda}\right) = p_c - \frac{Q}{\pi}\arccos\frac{(2d+\lambda)}{\lambda}. \tag{A16}$$

Thus, from Eqs.(A15), (A16) the flow topology in Fig. 2c and hodograph in Fig. 3c are realized if $p_c = p_{cc} = 0.8998$. If $p_c < p_{cc}$, we have the regime in Fig. 2b, 3b, which at even less p_c morphs into the regime in Fig. 2a, 3a.

The condition $\omega_1(-\lambda) = -\mathrm{i}v_0$ gives the magnitude of velocity at point O_1 for the regime in Fig. 2c:

$$v_0 = c\Big/\left(\int_{-\lambda}^{0}\frac{(2t-d)\mathrm{d}t}{\sqrt{|t|(d-t)(1-t)}} - 2\sqrt{\frac{\lambda(d+\lambda)}{1+\lambda}}\right) = 0.59. \tag{A17}$$

We recall that if Pluto's gravity is co-oriented with capillarity (Riesenkampf's flow from a zero-depth channel, PK-62) then $v_o > 1$ and the stronger capillarity (the larger p_c), the larger v_0.

In Fig. A2,a,b the flow net is plotted in accordance with formulas (A2), (A3), (A11). for $k = 1, L = 1, p_c = 0.8998$. The streamlines and equipotential lines are solid and dashed curves (correspondingly). The curve F_1E_1 in panel a) is the cap of CF. In panel b), the neighborhood of point $C = 1$ is zoomed.

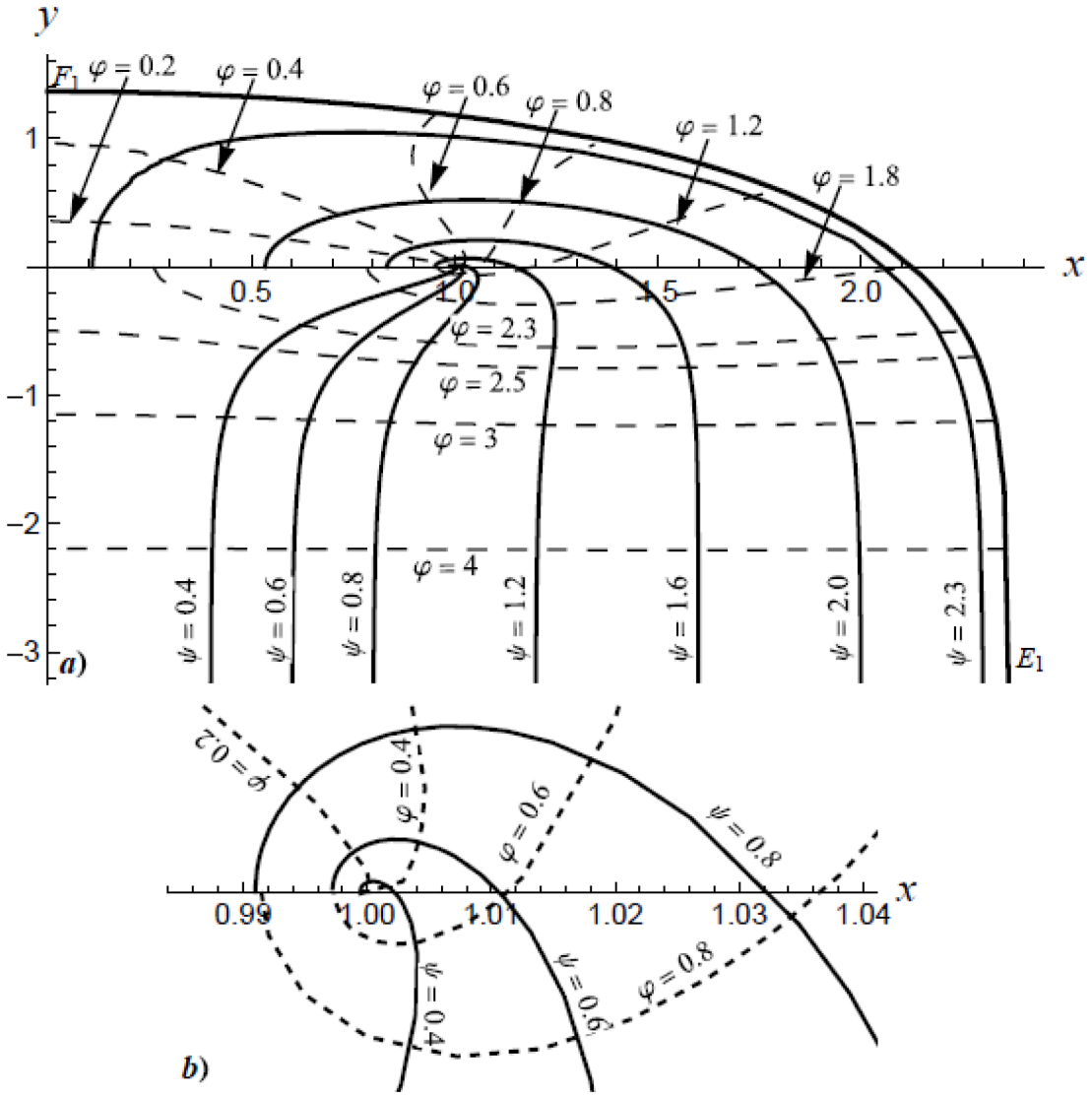

Fig. A2. a) Flow net for $k = 1$, $L = 1$, $p_c = 0.8998$; b) enlarged neighborhood of point $C = 1$.

Seepage topology with Philip's "dry wake" leeward of the liner

Now, we study the seepage regime in Fig. 2a and hodograph in Fig. 3a. The half-strip G_w and half-plane G_ζ are the same as for the "critical" case tackled above. The domain G_{ω_1} is a rectilinear trigon, which is easily made by the method of inversion (PK-62). We present only the final conformal mapping, an analogue of Eq. (A2):

$$\omega_1(\zeta) = A_m \int_0^\zeta \frac{\sqrt{\tau}\mathrm{d}\tau}{\tau - 1} = \frac{2}{\pi}\left(\sqrt{\zeta} - \operatorname{arctanh}\sqrt{\zeta}\right). \tag{A18}$$

The positive parameter in the Schwartz-Christoffel mapping, $A_m = 2/\pi$, is found from the condition that the jump of the imaginary part of function (A18) is -1 at the point $\zeta = 1$. At this point, the function $\mathrm{ArcTanh}\sqrt{\zeta}$ has a jump $i\pi/2$.

Using Eq. (A18) we obtain an analogue of Eq. (A11) in the physical complex domain:

$$z(\zeta) = \int_0^\zeta \frac{\mathrm{d}z}{\mathrm{d}w}\frac{\mathrm{d}w}{\mathrm{d}\tau}\mathrm{d}\tau + 1 = \frac{2Q_1\sqrt{d_1(d_1+\lambda_1)}}{\pi^2}\int_0^\zeta \frac{\sqrt{\tau} - \operatorname{arctanh}\sqrt{\tau}}{(d_1-\tau)\sqrt{\tau(\tau+\lambda_1)}}\mathrm{d}\tau + 1, \tag{A19}$$

where the flow rate Q_1 and the accessory parameters d_1, λ_1 have to be found (we add a subscript "1″ to these three quantities that distinguishes them from ones in the critical regime). The following three conditions are used. First, at point O_1 we have $z(-\lambda_1) = 0$, i.e.

$$\frac{2Q_1\sqrt{d_1(d_1+\lambda_1)}}{\pi^2}\int_{-\lambda_1}^0 \frac{\sqrt{|\tau|} - \arctan\sqrt{|\tau|}}{(d_1-\tau)\sqrt{|\tau|(\tau+\lambda_1)}}\mathrm{d}\tau = 1, \tag{A20}$$

Second, at point M_1 on the free surface

$$\frac{Q_1}{\pi}\operatorname{arcosh}\frac{2d_1+\lambda_1+\lambda_1 d_1}{\lambda_1(d_1-1)} = p_c \tag{A21}$$

The third and the last relation follows from the locus of point F_1, the apex of the CF:

$$\frac{2Q_1\sqrt{d_1(d_1+\lambda_1)}}{\pi^2}\int_{-\infty}^{-\lambda_1} \frac{\sqrt{|\tau|} - \arctan\sqrt{|\tau|}}{(d_1-\tau)\sqrt{\tau(\tau+\lambda_1)}}\mathrm{d}\tau = p_c - \frac{Q_1}{\pi}\operatorname{arccosh}\frac{(2d_1+\lambda_1)}{\lambda_1}. \tag{A22}$$

Eliminating $Q_1$from Eqs. (A20)-A22) we get the following system of two nonlinear equations for d_1 and λ_1:

$$\begin{aligned}
&\frac{2p_c\sqrt{d_1(d_1+\lambda_1)}}{\pi}\int_{-\lambda_1}^0 \frac{\sqrt{|\tau|} - \arctan\sqrt{|\tau|}}{(d_1-\tau)\sqrt{|\tau|(\tau+\lambda_1)}}\mathrm{d}\tau = \operatorname{arcosh}\frac{2d_1+\lambda_1+\lambda_1 d_1}{\lambda_1(d_1-1)},\\
&\frac{2\sqrt{d_1(d_1+\lambda_1)}}{\pi}\int_{-\infty}^{-\lambda_1} \frac{\sqrt{|\tau|} - \arctan\sqrt{|\tau|}}{(d_1-\tau)\sqrt{\tau(\tau+\lambda_1)}}\mathrm{d}\tau = \operatorname{arcosh}\frac{2d_1+\lambda_1+\lambda_1 d_1}{\lambda_1(d_1-1)} - \operatorname{arccosh}\frac{(2d_1+\lambda_1)}{\lambda_1}
\end{aligned} \tag{A23}$$

We solved system (A23) by the **FindRoot** routine of *Mathematica*.

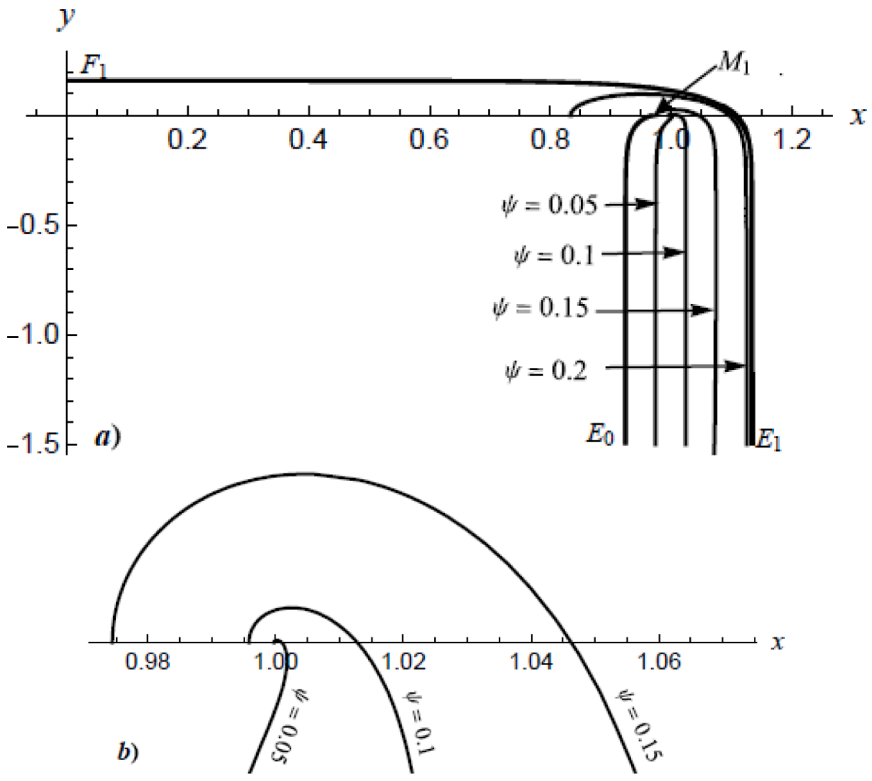

Fig. A3. a) Streamlines, including the right, F_1E_1, and left, M_1E_0, free boundaries sandwiching *CF* for $p_c = 0.16$; b) streamlines in the vicinity of point M_1.

As an example of the seepage regime with two free surfaces, we present the results for $p_c = 0.16$. The corresponding roots are $(d_1,\lambda_1) = (1.4392, 1.10261\times10^9)$. Then from Eq. (A21) $Q_1 = 0.2095$ and from Eq. (A19) at $\zeta = \xi = \infty$, we get $H = 0.15999$. The right and left solid lines in Fig. A3a shows the streamlines for $p_c = 0.16$, including two free boundaries, which bound the CF, viz. the curves F_1E_1 ($\psi = 0.2095$) and M_1E_0 ($\psi = 0$). The "dry wake" is on the left of M_1E_0. The "internal" streamlines are inidcated by arrows. All streamlines are plotted with the help of **Im, Re** and **ParametricPlot** routines of *Mathematica,* applied to Eq. (A19).

Fig. A3 demonstrates that capillarity makes a tension-saturated "fountain" above a zero-pressure line O_1C with a "free fall" (i.e. no backwater at infinity) and the Darcian leeward "dry wake". The free surface M_1E_0 creeps leftward under the horizontal no-flow liner, which subtends the emitting horizontal isobar. Due to 2-D seepage, the curve F_1E_1 is located below the "static horizontal limit" $y = p_c = 0.16$, which is attained at $L = \infty$. We recall that Vedernikov (1940) and PK-62 emphasized that the soil capillary constant p_c is determined for a static 1-D rise of CF above a horizontal water table (or in laboratory columns for sandy soils[5]). In dynamic situations, i.e. when seepage takes place, the apex of the CF is different from p_c, which in the Vedernikov-Bouwer model amalgamates Van Genuchten's WRC descriptors, *viz.* the dyad (α,n) used in Section 3. Smagin (2024) proved that at low volumetric moisture contents Van Genuchten's WRC should be devoid of a vertical asymptote, i.e. the finite values of p_c reported by PK-62 are, indeed, bounded from above (of course, on this planet for the existing value of $g = 9.81$ m/s^2 and atmospheric pressure near 100 kPa).

Obviously, at $y \to -\infty$ the distance between the vertical asymptotes of F_1E_1 and M_1E_0 in Fig. A2 equals Q, just as in the case of Riesenkampf's seepage from a zero-depth channel (PK-62).

We also plotted the whole flow nets and studies p_c values other than 0.16 (these results are dropped for the sake of brevity).

If the vertical asymptote of the free surface M_1E_0 attains the abscissa axis, i.e. if $x(E_0) = 0$ then one has to investigate the flow regime in Fig. 2b, with the hodograph in Fig. 3b. Such problem is rather cumbersome and we subterfuged it by recurring to HYDRUS2D. Mathematically, the dimensional p_c can be as large as one wishes. In case of very large p_c, one can interpret the flow regime in Fig. 2a as seepage into a bank of a shallow-depth water reservoir having $L = \infty$, the bottom of which is lined but the bank is not.

Data availability

No data was used for the research described in the article.

References

Abramowitz, M., Stegun, I.A., 1970. Handbook of Mathematical Functions. Dover, New York.

Akhmedov, A.D., Borovoy, E.P., Grigorov, M.S., Khodyakov, E.A., 2000. Subsurface Irrigation for the Cultivation of Forage Crops. Volgograd State Agricultural Academy, Volgograd (in Russian) АхМедов А.Д., Боровой Е.П., Григоров М.С., Ходяков Е.А., 2000. Внутрипочвенное орошение при возделывании корМовых культур. Волгоградская Государственная Сельскохозяйственная АкадеМия, Волгоград.

Al-Maktoumi, A., Al-Ismaily, S., Kacimov, A., Al-Busaidi, H., Al-Saqri, S., Al-Hadabi, M., 2014. Soil substrate as a cascade of capillary barriers for conserving water in a desert environment: lessons learned from arid nature. J. Arid. Land. 6, 690–703.

[5] For clayey soils, p_c can not be determined in such columns. Moreover, even field experiments above the water table in fine-textured aquifers (Muromtsev, 1991) give only assessments of the thickness of CF, because "stabilization" of CF in such porous media requires decades and the water table is not stable for decades, i.e. CF is "dynamic".

Al-Mayahi, A.K., Al-Ismaily, S.S., Breitenstein, D., Al-Busaidi, H.S., Al-Maktoumi, A.K., Lehmann, P., Or, D., Kacimov, A.R., Fahrni, S., Al-Shukaili, A.H., 2023. Soil water distribution and dynamics across prescribed capillary barriers under evaporating surfaces. Biosyst. Eng. 226, 55–70.

Astapov, S.V., Bobchenko, V.I., 1950. Subsoil-mole method of irrigation in the Central Chernozemregions. Hydrotech. Meliorat. 9, 41–52 (in Russian) Астапов С.В., Бобченко В.И., 1950. Подпочвенно-кротовый способ полива в Центрально-ЧерноземМных областях. Гидротехника и Мелиорация, N 9, 41-52.

Barashkov, V.I., 1980. Research on subsurface irrigation technology on light chestnut soils of the Volga-Don interfluve. In: Proceedings of the Volgograd Agricultural Institute, 70, pp. 68–77 (in Russian) Барашков, В.И., 1980. Исследования техники подпочвенного орошения на светло-каштановых почвах Волго-Донского МеЖдуречья. Труды Волгоградского Сельскохозяйственного Института. 70, 68-77.

Bobchenko, V.I., 1957. Subsurface Irrigation. Selkhozgiz, Moscow (in Russian) Бобченко В.И., 1957, ПодзеМное орошение. Сельхозгиз, Москва.

Bobchenko, V.I., 1959. Some results of the development of subsoil irrigation technology. In: Proceedings of the All-Union Scientific Research Institute of Hydraulic Engineering and Land Reclamation, pp. 36–49 (in Russian) Бобченко, В.И., 1959. Некоторые итоги разработки техники подпочвенного орошения. Труды Всесоюзного Научно-Исследовательского Института Гидротехники и Мелиорации, 36-49.

Boelter, D.H., Verry, E.S., 1977. Peatland and Water in the Northern Lake States (No. 31). USDA Forest Service, North Central Forest Experiment Station.

Bogushevsky, A.A., 1956. On some subsurface irrigation schemes. Hydrotech. Meliorat. 10, 27–32 (in Russian) Богушевский, А.А., 1956. О некоторых схеМах подпочвенного орошения. Гидротехника и Мелиорация, N 10, 27-32.

Bulakhtina, G.K., Kudryashov, A.V., Kudryashova, N.I., 2018. The influence of subsoil drip irrigation on the productivity of perennial grasses in the conditions of the Astrakhan region. Sci. Kuban 2, 31–35 (in Russian) Булахтина, Г.К., Кудряшов, А.В. and Кудряшова, Н.И., 2018. Влияние подпочвенного капельного орошения на продуктивность Многолетних трав в условиях севера Астраханской области. Наука Кубани, N 2, 31-35.

Deeb, M., Smagin, A.V., Pauleit, S., Fouché-Grobla, O., Podwojewski, P., Groffman, P.M., 2024. The urgency of building soils for Middle Eastern and North African countries: economic, environmental, and health solutions. Sci. Total Environ. 917, 170529. https://doi.org/10.1016/j.scitotenv.2024.170529.

Efimov, V.N., 1983. Peat Soils and Their Fertility. Agropromizdat, Leningrad (in Russian) ЕфиМов, В.Н., 1983. Торфяные почвы и их плодородие. АгропроМиздат. Ленинград.

El-Nesr, M.N., Alazba, A.A., Šimůnek, J., 2014. HYDRUS simulations of the effects of dual-drip subsurface irrigation and a physical barrier on water movement and solute transport in soils. Irrig. Sci. 32, 111–125.

Glebov, P.D., Dementyev, V.G., 1966. Prospects for the development of subsoil irrigation. Hydrotech. Meliorat. 8, 18–24 (in Russian) Глебов П.Д., ДеМентьев В.Г., 1966. Перспективы развития подпочвенного орошения. Гидротехника и Мелиорация. N 8. 18-24.

Gostishev, D.P., 1980. Experience in operating a subsurface irrigation site on floodplain lands. In: Proceedings of the Tashkent Scientific Research Institute of Agricultural Mechanization, 113, pp. 101–167 (in Russian) Гостищев, Д.П., 1980. Опыт эксплуатации участка внутрипочвенного орошения на пойМенных зеМлях. Труды Ташкентского Научно-Исследовательского Института Механизации Сельского Хозяйства, 113, 101-167.

Goyal, M.R. (Ed.), 2014. Sustainable Practices in Surface and Subsurface Micro Irrigation. Apple Academic Press, New York.

Grigorov, M.S., 1983. Subsoil Irrigation. Kolos, Moscow (in Russian) Григоров, М.С., 1983. Внутрипочвенное орошение. Колос, Москва.

Henrici, P., 1993. Applied and Computational Complex Analysis. Volume 3 Discrete Fourier Analysis, Cauchy Integrals, Construction of Conformal Maps, Univalent Functions. Wiley, New York.

Kacimov, A.R., Nicolaev, A.N., 1992. Steady seepage near an impermeable obstacle. *J. Hydrology* 138, 17–40.

Kacimov, A.R., Obnosov, Yu.V., 1995. Groundwater flow in a medium with periodic inclusions. Fluid Dyn. 30 (5), 758–766.

Kacimov, A.R., Obnosov, Yu.V., 2012. Analytical solutions for seepage near material boundaries in dam cores: the Davison-Kalinin problems revisited. Appl. Math. Model. 36, 1286–1301.

Kacimov, A.R., Obnosov, Y.V., 2017. Analytical solution for tension-saturated and unsaturated flow from wicking porous pipes in subsurface irrigation: the Kornev-Philip legacies revisited. Water Resour. Res. 53 (3), 2542–2552.

Kacimov, A., Obnosov, Yu.V., 2023. Phreatic seepage around a rectilinear cutoff wall: the Zhukovsky-Vedernikov-Polubarinova-Kochina dispute revisited. Adv. Water Resour. 173, 104367.

Kacimov, A.R., Obnosov, Y.V., Šimůnek, J., 2018. Steady flow from an array of subsurface emitters: kornev's irrigation technology and Kidder's free boundary problems revisited. Transp. Porous. Media 121, 643–664.

Kacimov, A.R., Obnosov, Y.V., Or, D., 2019. Evaporation-induced capillary siphoning through hydraulically connected porous domains: the Vedernikov–Bouwer model revisited. Transp. Porous. Media 129 (1), 231–251.

Kacimov, A., Obnosov, Yu.V., Šimůnek, J., 2022. Subterranean holes in the arid vadose zone as perturbations of descending pore water fluxes: J. R. Philip's legacy revisited. In: Sherif, M., Faiz, M.A., Sefelnasr, A. (Eds.), Abstracts of the International Conference "Water Resources Management and Sustainability: Solutions for Arid Regions", Dubai, March, 22-24, 2022, pp. 46–49.

Kacimov, A.R., 1992. Seepage optimization for a trapezoidal channel. J. Irrigat. Drain. Eng. ASCE 118 (4), 520–526.

Kacimov, A.R., 2000. Circular isobaric cavity in descending unsaturated flow. J. Irrigat. Drain. Eng. ASCE 126 (3), 172–178.

Kacimov, A.R., 2004. Capillary fringe and unsaturated flow in a reservoir porous bank. J. Irrigat. Drain. Eng. ASCE 130, 403–409.

Kacimov, A.R., 2006. Capillarity and evaporation exacerbated seepage losses from unlined channels. J. Irrigat. Drain. Eng. ASCE 132, 623–626.

Kacimov, A.R., 2007. Dipole-generated unsaturated flow in Gardner soils. Vadose Zone J. 6, 168–174.

Kalashnikov, A.A., Kalashnikov, P.A., Baizakova, A.E., 2014. Water-saving technology for subsoil irrigation of table beets. Sci. World 11 (15), 66–69 (in Russian) Калашников, А.А., Калашников,П.А., Байзакова, А.Е. 2014. Водосберегающая технология подпочвенного орошения столовой свеклы. *Science and World,* N 11 (15), 66-69.

Kanardov, V.I., 1979. Subsoil irrigation using small-diameter plastic pipes. Hydrotech. Meliorat. 6, 55–57 (in Russian) Канардов, В.И., 1979. Подпочвенное орошение с поМощью пластМассовых труб Малого диаМетра. Гидротехника и Мелиорация. N 6, 55-57.

Karpii, G.I., 1980. On the methodology for determining the parameters of subsoil humidifiers. Hydrotech. Meliorat. 10, 53–55 (in Russian) Карпий, Г.И., 1980. К Методике определения параМетров подпочвенных увлаЖнителей. Гидротехника и Мелиорация, N 10. 53-55.

Khamraev, N.R., 1974. Experience of subsurface irrigation in the Golodnaya Steppe. Hydrotech. Meliorat. 2, 53–56. ХаМраев, Н.Р., 1974. Опыт внутрипочвенного орошения в Голодной степи. Гидротехника и Мелиорация, N 2, 53-56.

Khamraev, N.R., 1980. Experience in the Construction of Subsurface Irrigation Systems. Kolos, Moscow (in Russian) ХаМраев, Н.Р., 1980. Опыт строительства системМ внутрипочвенного орошения. Колос, Москва.

Kichigin, V.N., 1958. Subsoil irrigation. Hydrotech. Meliorat. 2, 15–20. Кичигин, В.Н., 1958. Подпочвенное орошение. Гидротехника и Мелиорация, N 2, 15-20.

Kornev V.G., 1921. Способ и устройство для подпочвенного орошения с приМенениеМ труб. Патент СССР, N 139. Kornev V.G., 1921. Method and Device for Subsurface Irrigation Using Pipes. USSR patent N 139.

Kornev, V.G., 1935. Subsoil Irrigation (Absorption Irrigation Method). Selkhozgiz, Moscow (in Russian) Корнев В.Г., 1935. Подпочвенное орошение (Метод абсорбционного орошения). Москва, Сельхозгиз.

Lunev, V.N., Khondroyanis, Ya.E., 1975. Comparative effectiveness of subsurface irrigation in areas with different soil properties. In: Proceedings of the Central Asian Scientific Research Institute of Irrigation, 145, pp. 21–37 (in Russian) Лунев В.Н., Хондроянис Я.Е., 1975. Сравнительная эффективность внутрипочвенного орошения на участках с различныМи свойствааМи почвогрунтов. Труды Среднеазиатского Научно-Исследовательского Института Ирригации, Ташкент, 145, 21-37.

Mazepa, M.B., 1989. Distribution of irrigation rates in the soil profile during subsurface irrigation. Collection of Scientific Works of the Volgograd Agricultural Institute, pp. 33–39 (In Russian). Мазепа, М.В., 1989. Распределение поливных норМ в почвенноМ профиле при внутрипочвенноМ орошении. Сборник научных трудов Волгоградского Сельскохозяйственного Института, 33 - 39.

Muromtsev, N.A., 1979. The Use of Tensiometers in Soil Hydrophysics. Gidrometeoizdat, Leningrad (in Russian) МуроМцев, Н.А., 1979. Использование тензиоМетров в гидрофизике почв. Ленинград, ГидроМетеоиздат.

Muromtsev, N.A., 1991. Soil Hydrophysics for the Purpose of Reclamation. Gidrometeoizdat, Leningrad (in Russian) МуроМцев, Н.А., 1991. Мелиоративная гидрофизика почв. Ленинград, ГидроМетеоиздат.

Nasonov, V.G., Stanovov, G.N., 1978. Calculation of moisture contours for subsurface irrigation. In: Proceedings of the Central Asian Scientific Research Institute of Irrigation. Tashkent, 156, pp. 97–106 (in Russian) Насонов В.Г., Становов Г.Н., 1978. Расчет контуров увлаЖнения при внутрипочвенноМ орошении. Труды Среднеазиатского Научно-Исследовательского Института Ирригации, Ташкент, 156, 97-106.

Nikiforov, S.I., 1936. Subsoil irrigation. In: Proceedings of the All-Union Scientific Research Institute of Hydraulic Engineering and Land Reclamation, 17, pp. 5–82 (in Russian) Никифоров, С.И., 1936. Подпочвенное орошение. Труды Всесоюзного Научно-Исследовательского Института Гидротехники и Мелиорации, 17, 5-82.

Nikolaev, M.V., 1967. Experience in subsoil irrigation with wastewater. Hydrotech. Meliorat. 2, 57–65 (in Russian) Николаев, М.В., 1967. Опыт по подпочвенноМу орошению сточныМи водаМи. Гидротехника и Мелиорация, 2, 57-65.

Obnosov, Y.V., Kacimov, A.R., 2018. Steady Darcian flow in subsurface irrigation of topsoil impeded by a substratum: Kornev–Riesenkampf–Philip legacies revisited. Irrigat. Drain. 67 (3), 374–391.

Ostapchik, V.P., 1961. Subsoil irrigation system with pottery wetting. Hydrotech. Meliorat. 9, 14–23 (in Russian) Остапчик, В.П., 1961. СистеМа подпочвенного орошения с гончарныМи увлаЖнителяМи. Гидротехника и Мелиорация, N 9, 14-23.

Päivänen, J., 1973. Hydraulic conductivity and water retention in peat soils. Acta Forest. Finnica 143.

Philip, J.R., Knight, J.H., Waechter, R.T., 1989. Unsaturated seepage and subterranean holes: conspectus, and exclusion problem for circular cylindrical cavities. Water Resour. Res. 25 (1), 16–28.

Philip, J.R., 1989. Multidimensional steady infiltration to a water table. Water Resour. Res. 25, 109–116.

Polubarinova-Kochina, P.Ya., 1962. Theory of Ground-Water Movement. Princeton University Press, Princeton.

Radcliffe, D.E., Šimůnek, J., 2018. Soil Physics With HYDRUS: Modeling and Applications. CRC Press.

Readigger, V.P., 1965. Subsurface Irrigation by Mole Holes. Kolos, Moscow (in Russian) Ридигер В.Р. 1965. Подпочвенное орошение по кротовыМ дренаМ. Колос, Москва.

Samal, K.P., Mishra, G.C., 2017. Analysis of seepage from a triangular furrow considering soil capillarity using inverse hodograph and conformal mapping technique. ISH J. Hydraul. Eng. 23 (1), 1–12.

Samal, K.P. and Mishra, G.C., 2022. Analysis of seepage from parallel triangular Furrows by Inverse Hodograph and Conformal Mapping Technique. In Jha et al. (eds.), "*Hydrological Modeling*", Water Science and Technology Library 109, 459–478 https://doi.org/10.1007/978-3-030-81358-1_35, Springer.

Sheinkin, G.Yu., 1968. About subsoil irrigation. Cotton Grow. 3, 36–39 (in Russian) Шейнкин, Г.Ю., 1968, О подпочвенноМ орошении. Хлопководство, N 3, 36 - 39.

Shumakov, B.B., Aleksashenko, A.A., Gostishchev, D.P., 1985. Methodology for calculating the elements of equipment and the regime of intra-soil irrigation. Hydrotech. Meliorat. 8, 41–43 (in Russian) ШуМаков Б.Б., Алексашенко А.А., Гостищев Д.П., 1985. Методика расчета элеМентов техники и реЖиМа внутрипочвенного орошения Гидротехника и Мелиорация. N 8, 41 - 43.

Smagin, A.V., Sadovnikova, N.B., 2015. Creation of soil-like constructions. Euras. Soil Sci. 48 (9), 981–990. https://doi.org/10.1134/S1064229315090100.

Smagin, A.V., Sadovnikova, N.B., Belyaevaz, E.A., Krivtsova, V.N., Shoba, S.A., Smagina, M.V., 2022. Gel-forming soil conditioners of combined action: field trials in agriculture and urban landscaping. Polymers 14, 5131. https://doi.org/10.3390/polym14235131.

Smagin, A.V., Sadovnikova, N.B., Belyaeva, E.A., Korchagina, K.V., Krivtsova, V.N., 2023. Simulation modeling and practical use of the hydrological function of detritus in soil-engineering technologies. Moscow Univ. Soil Sci. Bull. 78 (4), 396–409. https://doi.org/10.3103/S0147687423040075.

Smagin, A.V., 2012. Soils Constructing: Theory and Practice. Moscow State University Press, Moscow (in Russian) СМагин А.В., 2012.Теория и практика конструирования почв. Издательство Московского Государственного Университета, Москва.

Smagin, A.V., 2024. Physically based thermodynamic model of the water retention curve of soils for the entire water range. Euras. Soil Sci. 57 (9), 1447–1460. https://doi.org/10.1134/S1064229324600234.

Strack, O.D.L., 1989. Groundwater Mechanics. Prentice-Hall, Englewood Cliffs.

Subramanya, K., Madhav, M.R., Mishra, G.C., 1973. Studies on seepage from canals with partial lining. J. Hydraul. Div. 99 (12), 2333–2351.

Suleiman, M.K., Shahid, S.A., 2024. Prospective of agricultural farming in Kuwait and Energy-Food-Water-Climate nexus. Terrestrial Environment and Ecosystems of Kuwait: Assessment and Restoration. Springer, Cham, pp. 363–391.

Swamee, P.K., Chahar, B.R., 2015. Design of Canals. Springer, New Dehli.

Vedernikov, V.V., 1936. The influence of soil capillarity on free-surface seepage. *Doklady AN SSSR*, III (12) 4 (99), 157–161. Ведерников, В.В., 1936. Влияние капиллярности грунта на фильтрацию со свободной поверхностью. Доклады АН СССР, III (12), N 4 (99), 157-161.

Vedernikov, V.V., 1939. Theory of Seepage and Its Applications to Problems of Irrigation and Drainage. Gosstroiizdat, Moscow (in Russian) Ведерников В.В.,1939. Теория фильтрации и ее приМенение в области ирригации и дренаЖа. Госстройиздат, Москва-Ленинград.

Vedernikov, V.V., 1940. Account of soil capillarity on seepage from a canal. Doklady AN SSSR 28 (5) (in Russian).

Wolfram, S., 1991. Mathematica. A System For Doing Mathematics By Computer. Addison-Wesley, Redwood City.

Yakovlev, N.P., Razuvaev, V.S., 1982. Subsoil irrigation with wastewater. Hydrotech. Meliorat. 4, 39–41 (in Russian) Яковлев, Н.П., Разуваев В.С., 1982. Подпочвенный полив сточныМи водаМи. Гидротехника и Мелиорация, N 4, 39-41.

Zakharov, R.Yu., Borbot, I.N., Skosar, D.V., 2021. On the feasibility of using subsurface irrigation in the Republic of Crimea. Econ. Construct. Environ. Manag. 81 (4), 53–63 (in Russian) Захаров, Р.Ю., Борбот, И.Н., Скосарь, Д.В., 2021. О целесообразности приМенения внутрипочвенного орошения в Республике КрыМ. ЭконоМика Строительства и Природопользования.

Zalibekov, Z.G., 2011. The arid regions of the world and their dynamics in conditions of modern climatic warming. Arid Ecosyst. 1, 1–7. https://doi.org/10.1134/S2079096111010094.

Zavodnov, S.S., Morozov, V.K., 1962. On the issue of regulating moisture during subsurface irrigation. Hydrotech. Meliorat. 1, 26–33 (in Russian) Заводнов, С.С., Морозов В.К., 1962. К вопросу регулирования увлаЖнения при подпочвенноМ орошении. Гидротехника и Мелиорация, N 1, 26-33.